Eur Heart J Cardiovasc Imaging Abstracts Supplement, December 2014
doi:10.1093/ehjci/jeu250

YOUNG INVESTIGATOR AWARD SESSION – BASIC SCIENCE

Thursday 4 December 2014, 10:00–11:00

Location: Agora

330

Contrast enhanced ultrasound molecular imaging of the inflammatory response in myocarditis

DC. Schmutzler[1]; E. Khanicheh[1]; L. Xu[2]; M. Mitterhuber[2]; K. Glatz[3]; E. Ellertsdottir[2]; BA. Kaufmann[1]
[1]University Hospital Basel, Cardiology, Basel, Switzerland; [2]University Hospital Basel, Department of Biomedicine, Basel, Switzerland; [3]University Hospital Basel, Pathology, Basel, Switzerland

Purpose: Cardiac tests for diagnosing myocarditis lack sensitivity or specificity. We hypothesized that contrast enhanced ultrasound molecular imaging (CEUMI) could detect endothelial inflammation and the recruitment of specific cellular components of the inflammatory response in murine myocarditis.
Methods: Microbubbles (MB) bearing antibodies targeting lymphocyte CD4 (MBCD4), endothelial P-Selectin (MBPSel), MB with a control antibody (MBCtr) and MB with a negative electrical charge for targeting of leukocytes (MBN) were prepared. Attachment of MBCD4 was validated in vitro with murine spleen CD4+ lymphocytes. 20 mice were studied after induction of autoimmune myocarditis by immunisation with α-myosin-peptide, 20 mice served as controls. CEUMI of the heart was performed with MBCD4, MBPSel, MBN, and MBCtr. Left ventricular ejection fraction (LVEF) and circumferential strain (CS) were measured. A pathologist blinded to all other data graded the severity of myocarditis on a scale from 0 (no myocarditis) to 4 on histology. Animals were grouped into NM (no myocarditis), MM (moderate myocarditis, score 1-2) and SM (severe myocarditis, score 3-4).
Results: In vitro, attachment of MBCD4 to CD4+ lymphocytes was significantly greater than MBCtr ($p<0.01$). LVEF did not differ between groups (NM 71 $\pm$ 13%, MM 73 $\pm$ 7%, SM 62 $\pm$ 20%, $p=0.5$), nor did CS (NM 36 $\pm$ 9%, MM 25 $\pm$ 11%, SM 30 $\pm$ 7%, $p=0.4$). CEUMI (figure) showed increased signal for targeted MB vs MBCtr in MM and SM, whereas signals in NM did not differ from MBCtr.
Conclusions: CEUMI can detect endothelial inflammation and leukocyte infiltration in myocarditis, while functional imaging fails to do so. In particular, imaging of CD4+ lymphocytes involved in autoimmune responses in myocarditis is possible. CEUMI may be a powerful method for assessing myocarditis.

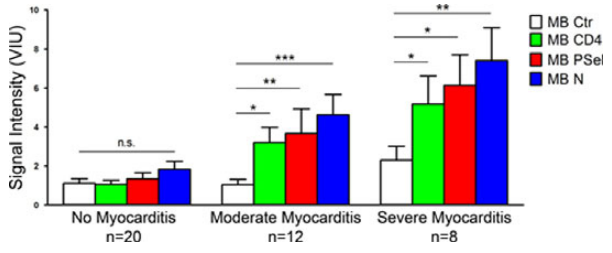

Abstract 330 Figure. CEUMI in Myocarditis (mean $\pm$ SEM)

331

Molecular imaging of inflamed atherosclerotic plaque with 18F-anti-VCAM-1 nanobody and PET/CT

G. Bala[1]; A. Blykers[2]; C. Xavier[2]; K. Gillis[1]; S. Tierens[2]; B. Descamps[3]; C. Vanhove[3]; T. Lahoutte[4]; B. Cosyns[1]; S. Hernot[2]
[1]University Hospital (UZ) Brussels, Centrum voor Hart-en Vaatziekten - CHVZ, Brussels, Belgium; [2]Free University of Brussels (VUB), In Vivo Cellular and Molecular Imaging – ICMI, Brussels, Belgium; [3]Ghent University, iMinds-IBiTech-MEDISIP, Department of Electronics and Information Systems,, Ghent, Belgium; [4]University Hospital (UZ) Brussels, Nuclear Medicine, Brussels, Belgium

Purpose: Vascular cell adhesion molecule-1 (VCAM-1) is expressed in inflammatory atherosclerotic lesions and is a potential target for the molecular imaging of vulnerable plaques. A mouse/human cross-reactive anti-VCAM-1 nanobody (Nb) radiolabeled with 99mTc has previously demonstrated to allow detection of VCAM-1 positive plaques using SPECT/CT. Because of its superior spatial resolution, higher sensitivity, and more accurate quantification, Positron Emission Tomography (PET) is more appropriate for clinical use. Therefore, we aimed to validate the 18F-labeled anti-VCAM-1 Nb as a potential PET tracer and show its ability to image VCAM-1 expression by PET/CT in a mouse model of atherosclerosis.
Methods: The anti-VCAM-1 Nb (cAbVCAM1-5) was labeled using the prosthetic group N-succinimidyl-4-18F-fluorobenzoate (18F-SFB) and purified by size exlusion chromatography. In vitro cell binding studies using TNF-α stimulated bEND5 cells were carried out to assess the functionality of the tracer. In vivo μPET/CT imaging was performed at 2h30 post-injection using 20-30 weeks-old ApoE$-/-$ mice on a Western diet (Group 1) and normally fed C57BL6 control mice (n=3 per group), which were injected with 18F-anti-VCAM-1 Nb. To demonstrate the specificity, additional ApoE$-/-$ mice were injected with 18F-labeled non-targeting control Nb or with 70-fold excess of unlabeled anti-VCAM-1 Nb. Ex-vivo evaluation (n=6 per group) of plaque uptake in different aorta segments based on lesion-extension index was assessed by using gamma well counting.
Results: After 18F-labeling (radiochemical purity >99%), 18F-labeled anti-VCAM-1 Nb showed significantly more binding to VCAM-1 positive cells compared to negative cells. Atherosclerotic lesions in the aortic arch of ApoE$-/-$ mice injected with 18F-anti-VCAM-1 Nb were successfully identified using μPET/CT imaging, while background signal was observed in the aortic arch of the control groups. These results were confirmed by ex vivo analysis where uptake of 18F-anti-VCAM-1 Nb was significantly higher compared to control groups and increased with the lesion-extension index (score 0: 0.68 $\pm$ 0.10, score 1: 1.18 $\pm$ 0.36, score 2: 1.49 $\pm$ 0.37, score 3: 1.48 $\pm$ 0.38 %ID/g). In the Group 1, lesion-to-heart and lesion-to-blood ratios were high (11.2 and 3.13, respectively).
Conclusion: Mouse/human 18F-anti-VCAM-1 Nb allows non-invasive PET/CT imaging of VCAM-1 expression in atherosclerotic plaques in a mouse model and may represent an attractive tool for imaging vulnerable atherosclerotic plaques in patients.

332

Strain and strain rate correctly identify myocardial dysfunction in advanced glycation end products (AGEs) injected rats

V. Ferferieva[1]; D. Deluyker[1]; T. Arslan[1]; I. Lambrichts[2]; JM. Rigo[1]; V. Bito[1]
[1]Hasselt University, Department of physiology, BIOMED, Diepenbeek, Belgium; [2]Hasselt University, Department of morphology, BIOMED, Diepenbeek, Belgium

Purpose: Advanced glycation end products (AGEs) are known to play a key role in the development and progression of cardiovascular diseases, however, the precise underlying mechanism still remains elusive. The study was therefore established to identify the role of AGEs in the pathophysiology of heart failure.
Methods: 13 Sprague-Dawley rats underwent a daily injection of 20 mg/kg BSA-modified AGEs (n=9) or control-BSA (n=4) for 6weeks. 2D echo at baseline (BL) and 6w follow-up was used to calculate LV dimensions, volumes (EDV, ESV) and sphericity index (SI). Circumferential strain (Scirc) and strain rate (SRcirc) were obtained at mid-ventricular level using speckle tracking imaging (STI). LV fibrosis was measured using Sirius Red staining.
Results: After AGEs injection, a progressive LV remodeling was observed with increased posterior and anterior wall thicknesses, along with higher EDV, ESV and SI compared to BL (0.26 $\pm$ 0.1mL vs 0.15 $\pm$ 0.02mL; 0.09 $\pm$ 0.05mL vs 0.04 $\pm$ 0.01mL and 0.3 $\pm$ 0.04 vs 0.18 $\pm$ 0.03 $p<0.05$). Ejection fraction and fractional shortening did not change over

time, whereas both systolic Scirc/SRcirc were significantly decreased (-16.4 ± 1.8 vs -21.6 ± 2.7% and -4.7 ± 1.0 vs -6.7 ± 0.7 1/s, $p<0.05$). Myocardial fibrosis was significantly increased compared to BSA-injected animals and was associated with decreased Scirc/SRcirc (figure1).

Conclusion: AGEs injection was associated with prominent cardiac remodelling and increased myocardial fibrosis. STI-derived S/SRcirc correctly detect myocardial dysfunction secondary to increased AGEs and might be useful parameters to monitor the effect of new therapeutic strategies preventing the myocardial dysfunction associated with AGEs.

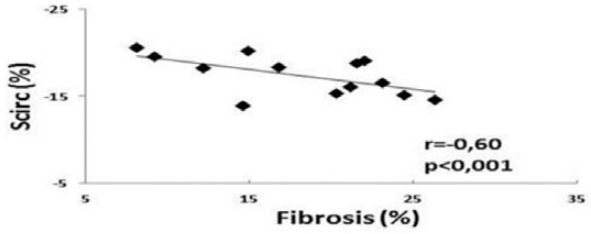

Abstract 332 Figure.

333

Structural and functional Right Ventricular remodeling is related to training intensity in an experimental model of endurance exercise

M. Sanz[1]; M. Sitges[1]; B. Bijnens[2]; C. Rubies[3]; M. Batlle[3]; LL. Mont[1]; J. Brugada[1]; E. Guasch[1]

[1]Barcelona Hospital Clinic, Barcelona, Spain; [2]ICREA, Institució Catalana de Recerca i Estudis Avançats, Barcelona, Spain; [3]Institute of Biomedical Research August Pi Sunyer (IDIBAPS), Barcelona, Spain

Background: Recent data has shown specific remodeling of the right ventricle (RV) in response to chronic training, especially in endurance sport. However, it is not known if this adaptation is related to the intensity of training or if there is a threshold for developing this adverse remodeling beyond the normal physiologic response. The aim of this study was to use an animal model to evaluate the relationship between RV remodeling and intensity of training.

Methods and Results: 36 Wistar rats were conditioned to run daily in a treadmill at a moderate (Mod, 45 min at 30cm/s) or vigorous (Vig, 60 min at 60cm/s) intensity for 16 weeks; Sedentary rats (Sed) served as controls. Echocardiography was performed at the 16th week. Analysis consisted on standard echocardiography of both ventricles,including dimensions, systolic and diastolic function and Tissue Doppler Imaging echocardiographic assessment of the RV.Both ventricles similarly dilated (roughly 15%) after Mod training. Mod rats developed improved RV function by increasing RV apical function, whithout changes in LV function. With Vig training, though, a decline in RV mid-basal systolic function,RV diastolic function and a disproportionally enlarged RV were observed.

Conclusion: In this animal model, moderate endurance exercise caused favourable remodeling of the RV. However, vigorous training caused a deleterious remodeling, with RV dilatation, decreased contractility and worse diastolic function. Our finding suggests that there might be a threshold with intense training from which cardiac adaptation might start to be deleterious. Whether these changes are reversible should be further investigated.

Abstract 333 Table. RV and LV measures in the 3 groups

	Group Sed N=17	GroupMod N=19	GroupVig N=17	Anova Test (p)
RVDA(mm2/g)	69,5 ± 8,8	80,4 ± 9,6	88,0 ± 9,2	<0,01
RV mid-apical free wall SR (s^{-1})	2,9 ± 0,5	3,3 ± 0,6	3,0 ± 0,4	0,04
RV basal free wall SR (s^{-1})	3,3 ± 0,8	3,3 ± 0,7	2,7 ± 0,6	0,04
RVIRT /HR ((ms.min/ beats)x100)	4,2 ± 0,9	4,3 ± 1,0	5,3 ± 1,4	0,03
LVDd (mm/g)	15,3 ± 2,0	18,3 ± 1,4	18,5 ± 1,6	<0,01
LVEF (%)	78,6 ± 4,6	79,6 ± 1,6	80,7 ± 1,4	0,14
LVIRT /HR ((ms.min/ beats)x100)	4,7 ± 1,0	5,0 ± 1,0	5,2 ± 1,0	0,32

RVDA: Right Ventricular end-Diastolic AreaRVIRT: Right Ventricular Isovolumetric Relaxation TimeLVIRT : Left Ventricular Isovolumetric Relaxation Time